

Electronic Supplementary Material (ESI) for Lab on a Chip

Efficient single-cell poration by microsecond laser pulses

Qihui Fan,^a Wenqi Hu^b and Aaron T. Ohta^{*b}

Part I. Cells exposed to laser light without microbubble

In order to exclude the damage and cell poration function caused by laser light other than oscillating microbubble activity, a test was designed and conducted to check for cell poration and cell viability in the presence of laser light, but without microbubbles. In this negative control test, a clear glass slide was used as the bottom of the fluidic chamber, replacing the optically absorbent substrate. All other procedures were the same as in the common cell poration and cell viability tests. In this setup, much more light reaches the cell under poration; nonetheless, the targeted cells did not show any red fluorescence, indicating the cells were not damaged by the laser (Fig. S1). The cells also did not display any green fluorescence, indicating that poration does not occur if cells are merely exposed to laser with no microbubbles present.

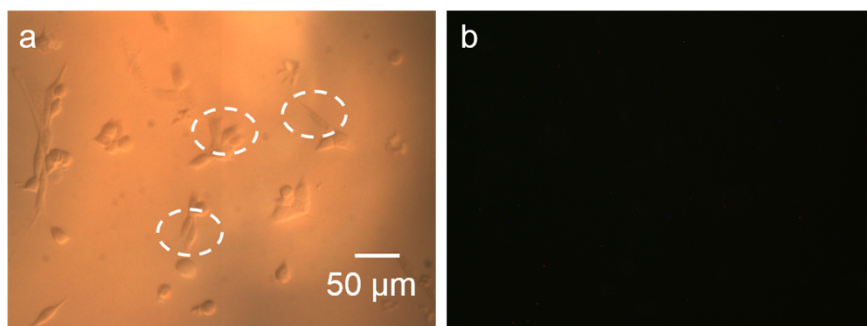


Fig. S1 Cell poration and cell viability when the optically absorbent substrate is replaced with clear glass slide. In this setup, the cells are exposed to the laser, but there is no microbubble present. (a) Optical microscopic image. The target cells are marked by dashed circles. (b) No green or red fluorescence from FITC or PI was present under fluorescent microscopy, indicating that no cell poration or cell death occurred.

Part II. Microstreaming surrounding size-oscillating bubbles

The microstreaming around the size-oscillating bubble was visualized using 0.5- μm polystyrene beads as tracer particles. The oscillating bubble was induced with a 60- μs laser pulse width. The toroidal flow profile displayed by the submicron tracer particles extends 20 to 30 μm from the center of the bubble (Fig. S2). This image is a composite of 66 images recorded over 1 second, processed using ImageJ software.

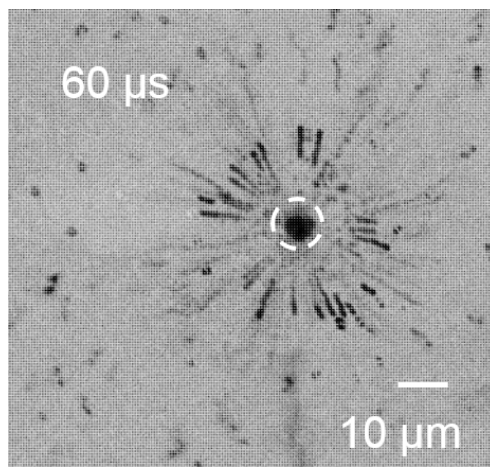


Fig. S2 Microstreaming around an oscillating bubble visualized with tracer particles (0.5- μm -diameter polystyrene beads). This is a composite of 66 images taken over 1 second. The bubble is marked by the dashed circle.

More quantitative microstreaming measurements were conducted with a 10- μm -diameter polystyrene bead. The horizontal and vertical displacement of the tracer bead was recorded, mapping the motion of the tracer bead in the toroidal flow around the 60- μs laser pulse-induced oscillating bubble. The displacement in vertical direction (z -displacement) of the bead can be determined by measuring the brightness at the center of the microbead.¹ The centroid brightness for the bead was recorded for different z -direction displacements, by adjusting the specimen stage of the microscope using a Vernier micrometer (SM-25, Newport). The brightness of the image at the center of the bead was measured using ImageJ software, and correlated to the z -direction displacement. The calibration of the z -displacement versus centroid brightness is demonstrated in Fig. S3a.

The bead positions in the microstreaming was recorded every 17 ms (Fig. S3b). The trajectory of

the tracer bead in the r - z plane shows the microstreaming around the oscillating microbubble. Each circle in Fig. S3b marks the bead position at each frame. The bead trajectory indicates that when the bead was 25 to 30 μm away from the oscillating bubble, the bead begins to move towards the bubble at an increasing rate. When the bead was close to the bubble center, the microstreaming in the vertical direction moved the tracer bead rapidly to the top of the chamber. The bead moved from a position near the substrate to a position in the upper circulatory flow within one frame step, or within an interval of 17 ms. Subsequently, the bead was pushed away from the bubble center by the microstreaming, at rate that decreased with distance from the bubble. The calculated instantaneous horizontal velocity of the 10- μm tracer bead is shown in Fig. S3c. Negative velocities correspond to bead movement towards the bubble. Due to the limited frame rate, it cannot be known if the z -displacement of tracer bead occurs in less than 17 ms. Assuming the z -displacement of the bead takes the entire 17 ms, the vertical velocity of the bead can be estimated to be 898 $\mu\text{m/s}$.

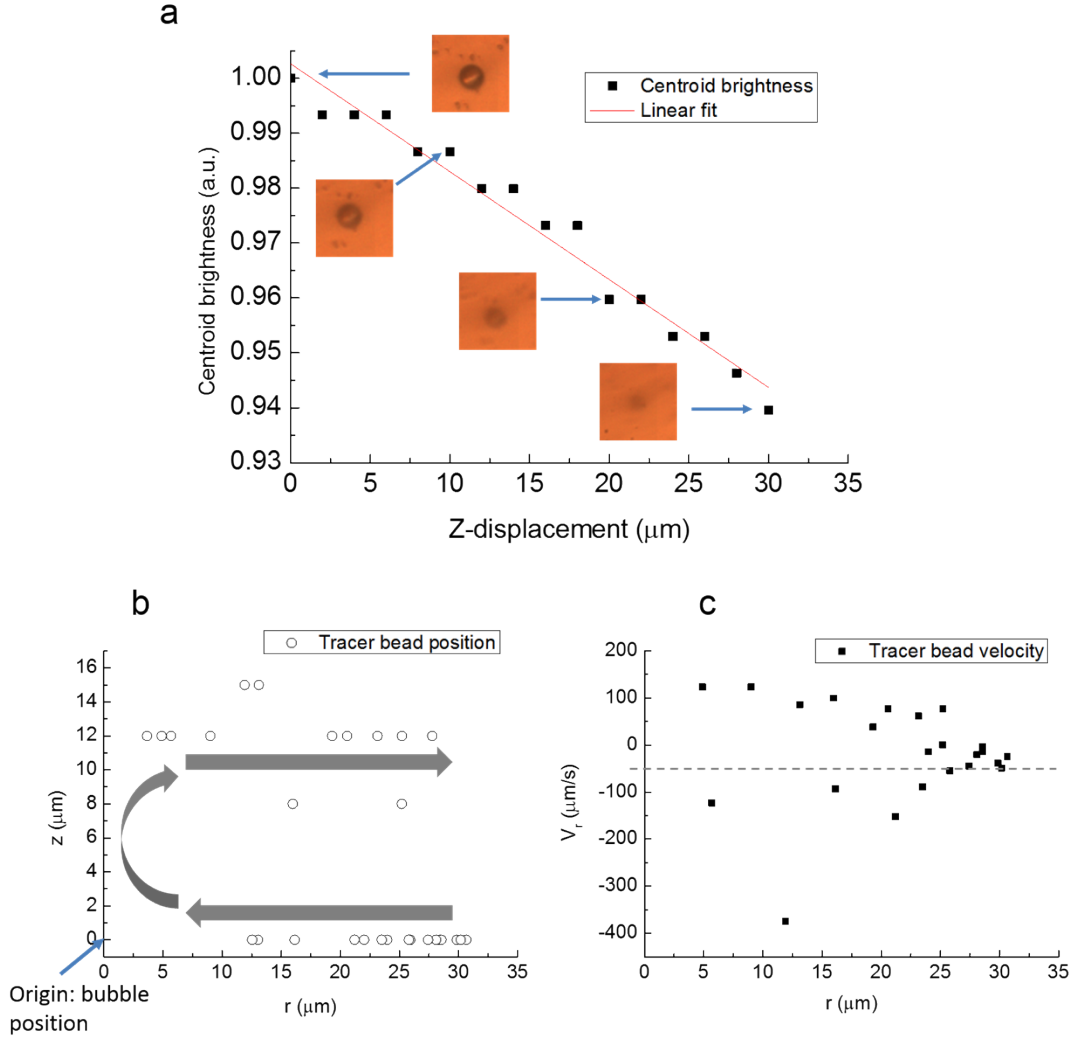


Fig. S3. Quantitative study of the toroidal flow by a 10-μm tracer bead. (a) z -displacement of the tracer bead versus the measured brightness of the bead centroid. (b) The position of the 10-μm tracer bead shows the motion of the toroidal flow in the r - z plane. The grey arrow shows the direction of the bead movement, and the bubble center is at the origin. The bead positions are recorded every 17 ms. (c) The measured horizontal (V_r) instantaneous velocity of the bead as a function of horizontal displacement along the r -direction. The laser pulse width was 60 μs.

Part III. Characterization results and discussion for scanning-laser mode

1. Laser scanning speed

The scanning speed of laser is one of factors affecting the cell poration performance in scanning-laser mode. If the laser moves too rapidly, there is insufficient bubble-cell interaction for poration; if the laser moves too slowly, the prolonged bubble-cell interaction may damage the cell. As shown in Fig. S4, when the laser scanning speed was 50 $\mu\text{m/s}$, both the poration efficiency and cell viability are $95.1 \pm 3.0 \%$, meaning that the poration is limited only by the amount of cells that are viable. If the laser speed is decreased to 12 $\mu\text{m/s}$, the cell viability is reduced to $50.0 \pm 10.8 \%$, and the cell poration efficiency is also limited to $45.0 \pm 8.7 \%$. If the laser scanning speed is increased to 120 $\mu\text{m/s}$ and 200 $\mu\text{m/s}$, the poration efficiency was decreased to $60.0 \pm 10.0 \%$ and $16.7 \pm 3.3 \%$, respectively, while the cell viabilities were maintained at 100 %.

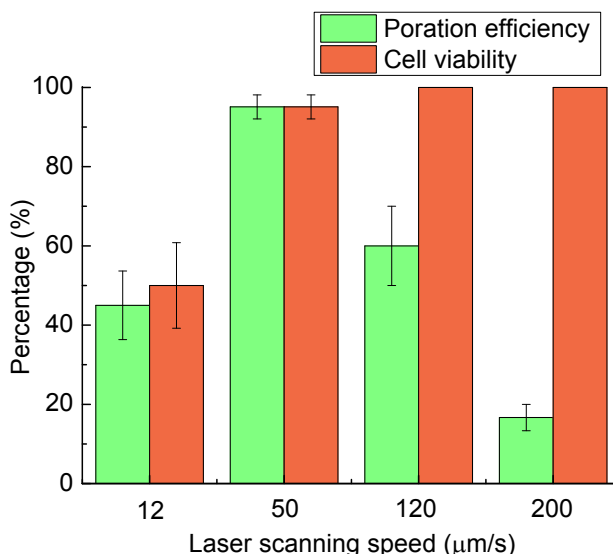


Fig. S4. Cell poration efficiency and cell viability as a function of the laser scanning speed. Error bars show the standard error of the measurements. More than 30 cells were tested in three parallel experiments for each laser scanning speed.

2. Fluidic chamber height for the scanning-laser mode

The fluidic chamber height dictates the vertical working distance between the edge of the microbubble and the cell membrane. This affects the maximum shear stress at the cell membrane

from the microstreaming surrounding the microbubble. The shear stress decreases rapidly as the distance from the microbubble increases.^{2, 3} The shear stress was too strong at a chamber height of 10 μm , so this caused damage to the cells. This resulted in reduced cell viability, and thus also affected the poration efficiency (Fig. S5). The strength of the shear stress is reasonable for a chamber height of 20 μm , which provides both a poration efficiency and a cell viability of 95.1 ± 3.0 %. A chamber height of 25 μm maintains the high cell viability, but the cell poration efficiency decreases to 56.7 ± 8.8 %, which can be attributed to a reduction in the shear stress at the cell membrane. The shear stress continues to weaken as the chamber height increases to 30 μm , resulting in no observable poration. Therefore, the 20- μm chamber height was selected as the best combination of poration efficiency and cell viability.

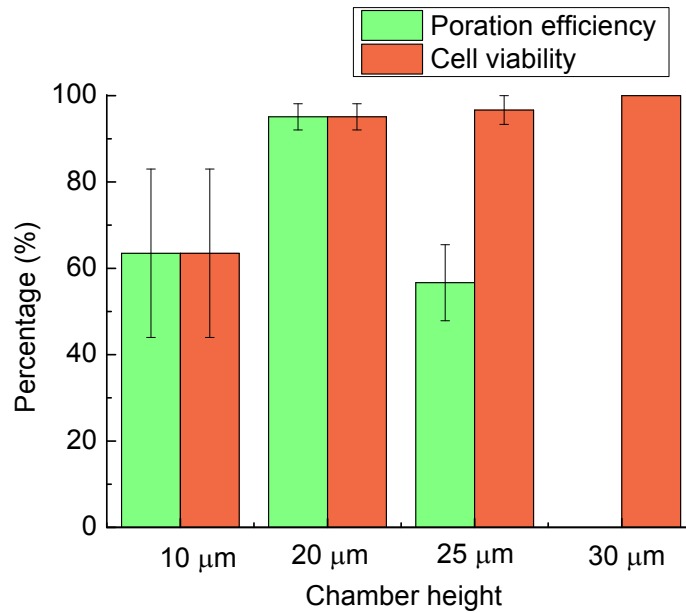


Fig. S5 Cell poration efficiency and cell viability as a function of chamber height in the scanning-laser mode. Error bars show the standard error of the measurements. More than 30 cells were tested in three parallel experiments for each chamber height.

References

1. W. Hu, Q. Fan and A. T. Ohta, *Lab Chip*, 2013, **13**, 2285-2291.
2. A. N. Hellman, K. R. Rau, H. H. Yoon and V. Venugopalan, *J Biophotonics*, 2008, **1**, 24-35.
3. Q. Fan, W. Hu and A. T. Ohta, *Lab Chip*, 2014, **14**, 1572-1578.